Assessment and prediction of dust emissions, deposition and radiation forcing in Central Asia

Ying gan[123]， Zhe Zhang[1234*], Wen Chu[5]， Jianli Ding[6]， Yuxin Ren[123]

1College of Geography and Remote Sensing Sciences, Xinjiang University, Urumqi, 830046, China

2 Xinjiang Key Laboratory of Oasis Ecology, Xinjiang University, Urumqi, 830046, China

3 Key Laboratory of Smart City and Environment Modelling of Higher Education Institute, Xinjiang University, Urumqi, 830046, China

4MNR Technology Innovation Center for Central Asia Geo-Information Exploitation and Utilization, Urumqi, 830046, China

5College of Marine Technology, Faculty of Information Science and Engineering；Ocean University of China；Qingdao；266100

6Xinjiang Institute of Technology, Aksu, China;

* *Correspondence to: zhangzhe_0110@yeah.net；Tel:86+18799181249*

S1. SBDART with solar photometer verification

Our study, conducted with thoroughness and precision, aims to more accurately evaluate the quality of the direct radiative forcing (ADRF) data calculated by the SBDART radiation transfer model in Central Asia. We comprehensively compare and analyze the radiation flux data at each site simulated by the SBDART model with the upward and downward radiation fluxes in the radiative forcing provided by the solar photometer observation network.

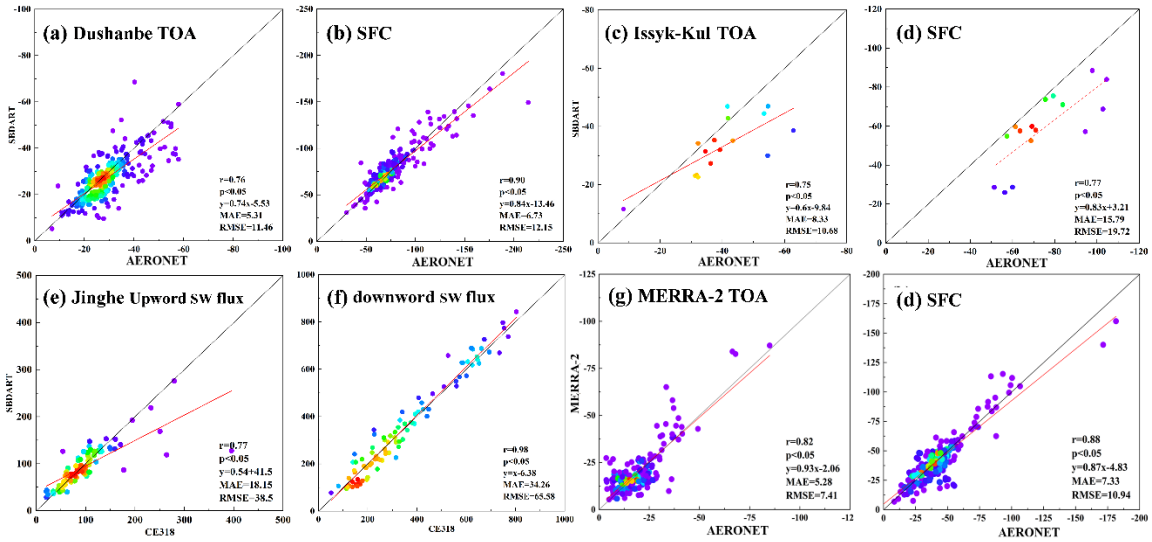

Fig. S1. Linear fits of short-wave radiation fluxes obtained by SBDART, MERRA-2 and the solar photometer.

S2.Historical spatial distribution of dust emissions and deposition under different CMIP6 scenarios

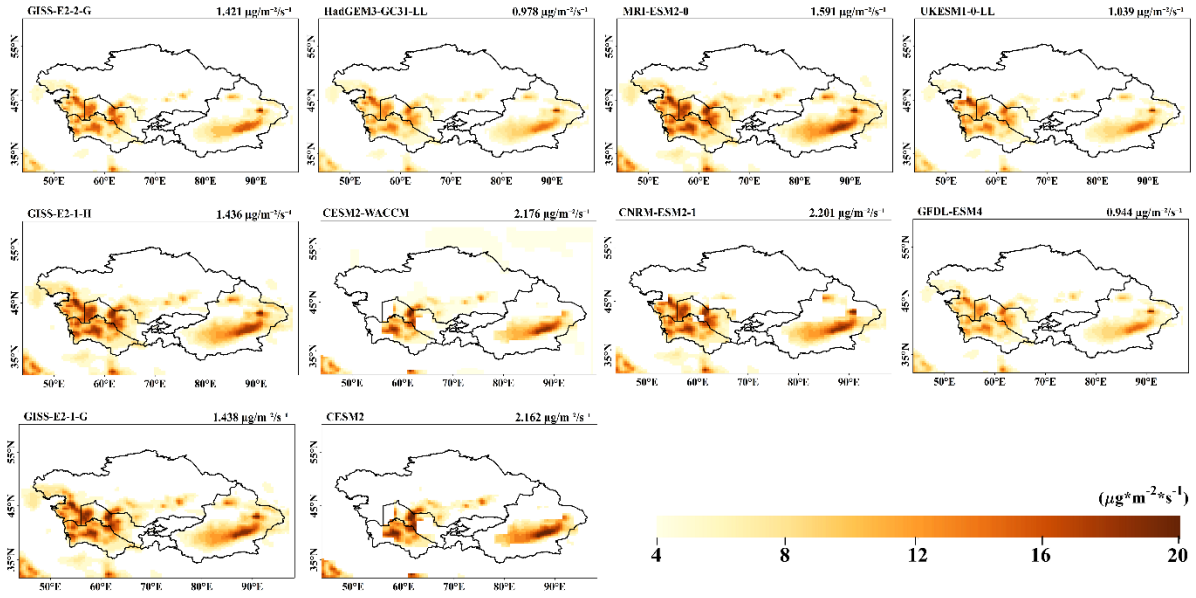

Fig. S2. Historical spatial distribution of sand and dust emissions in Central Asia under 10 CMIP6 models.

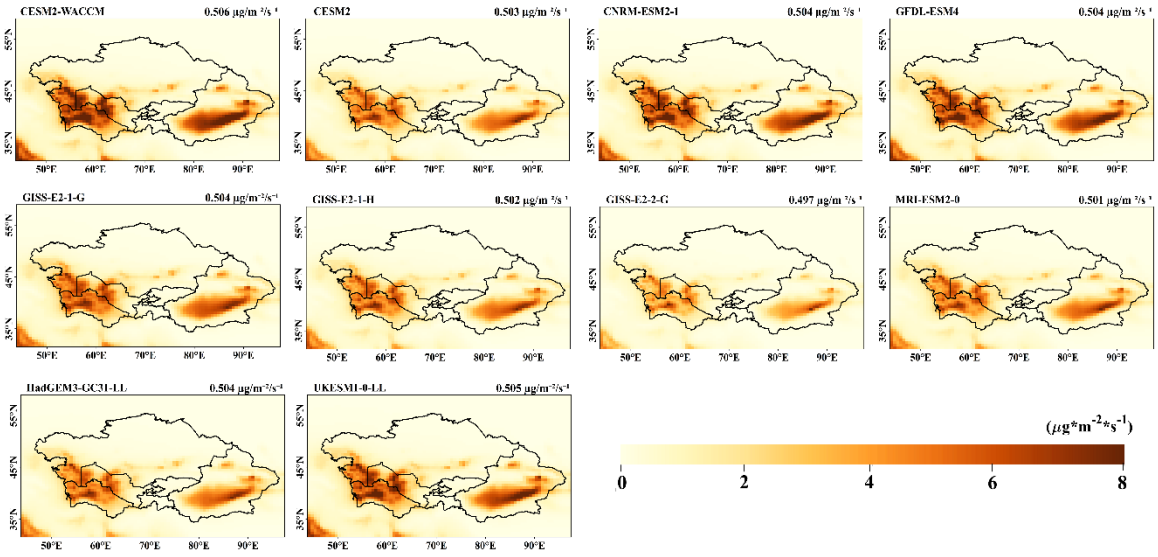

Fig. S3. Historical spatial distribution of dry deposition of sand and dust in Central Asia in 10 CMIP6 models.

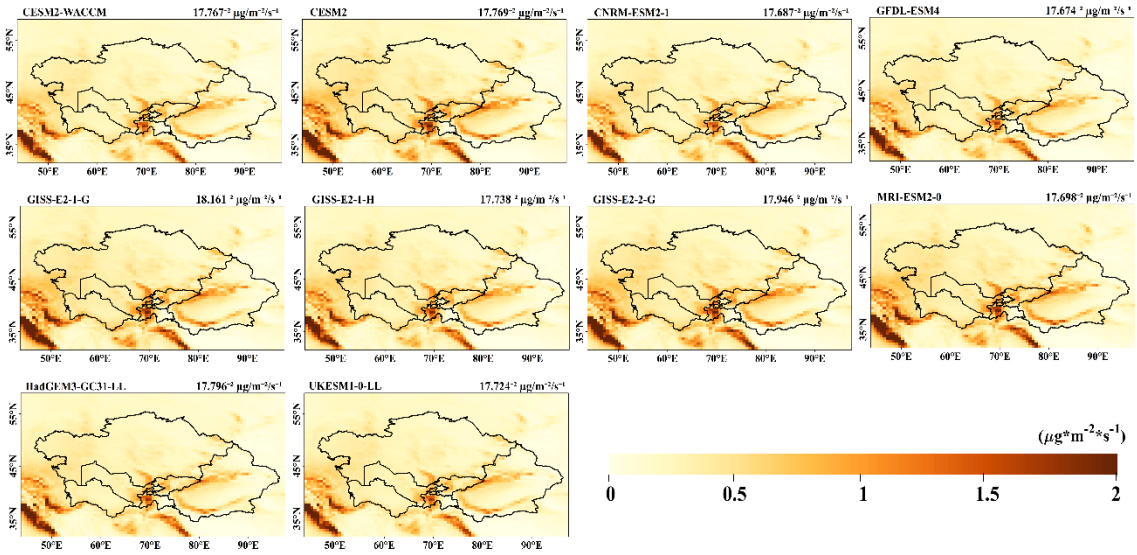

Fig. S4. Historical spatial distribution of wet deposition of sand and dust in Central Asia under 10 CMIP6 models

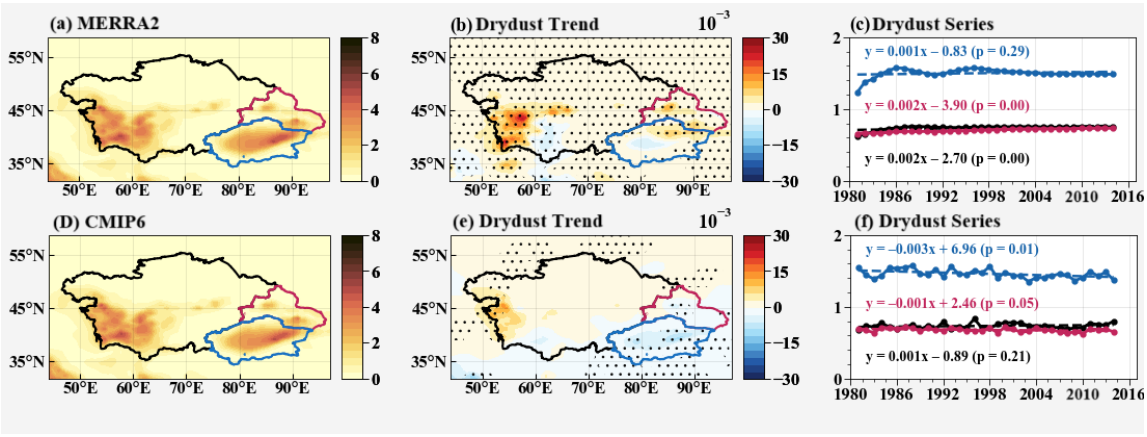

Fig. S5. Spatial distribution, linear trend, and time series of dry deposition of sand and dust from MERRA-2 and CMIP6 MME in Central Asia from 1980 to 2014. Red highlights the area north of Xinjiang, blue indicates the south of Xinjiang, and black indicates the Central Asian five countries (b) and (e). The black dots indicate the area with a confidence level of 90%.

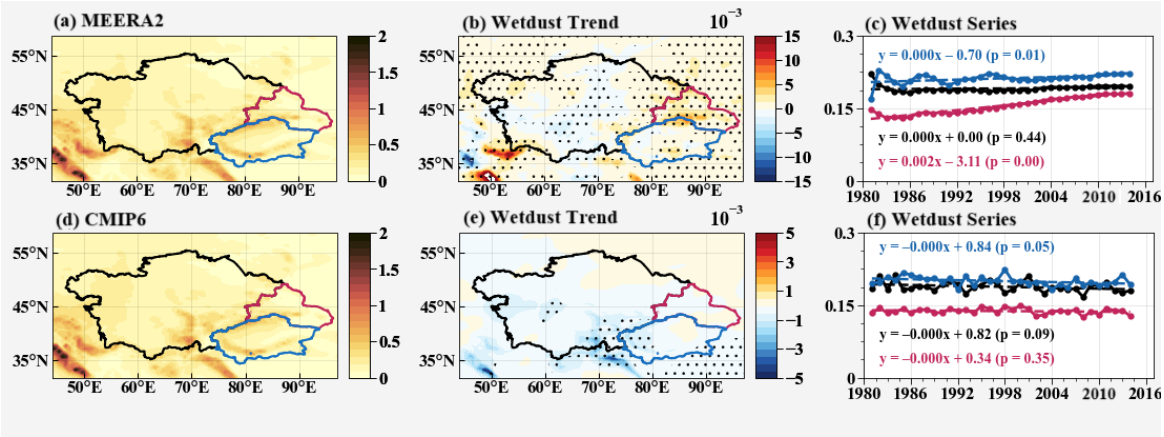

Fig. S6. Spatial distribution, linear trend, and time series of wet deposition of sand and dust from MERRA-2 and CMIP6 MME in Central Asia from 1980 to 2014. Red highlights the area away from the northern Xinjiang region, blue indicates southern Xinjiang, and black indicates the Central Asian five countries (b) and (e). The black dots indicate the area with a confidence level of 90%.

S3. Future projections of wet and dry deposition based on the CMIP6 multimodel ensemble mean

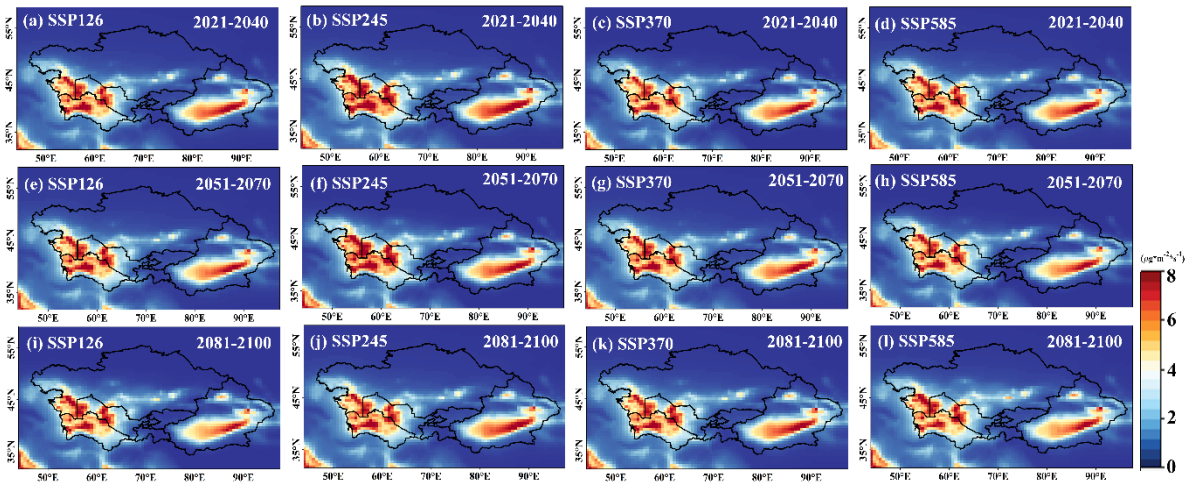

Fig. S7. Future changes in dry deposition of sand and dust at different times. Spatial variations of dust-dry deposition in Central Asia under the four CMIP 6 MME SSP scenarios for (a–d) the recent period (2021–2040), (e–h) the medium term (2051–2070), and (i–l) the long term (2081–2100) relative to the historical period (2000–2014).

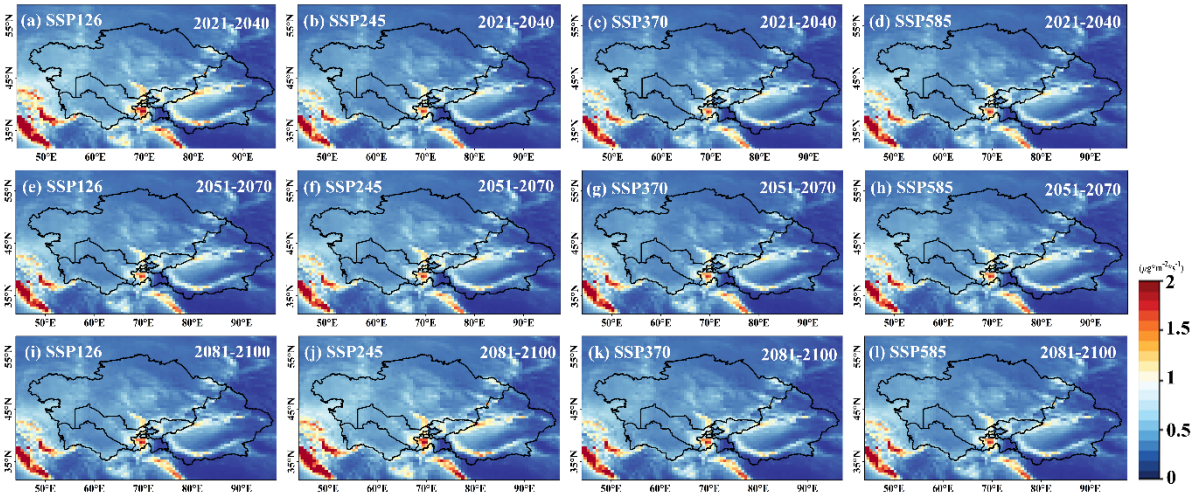

Fig. S8. Future changes in wet deposition of sand and dust at different times. Spatial variations of wet dust deposition in Central Asia under the four CMIP 6 MME SSP scenarios for (a–d) the recent period (2021–2040), (e–h) the medium term (2051–2070), and (i–l) the long term (2081–2100) relative to the historical period (2000–2014).

S4. SARIMA model prediction of direct radiation forcing of sand and dust aerosols

In order to simplify the content of the appendix, this study selected five sample diagnostic maps from the southern Xinjiang region as examples in the appendix. The results of the maps in other regions are similar. For specific data, please refer to the appendix.

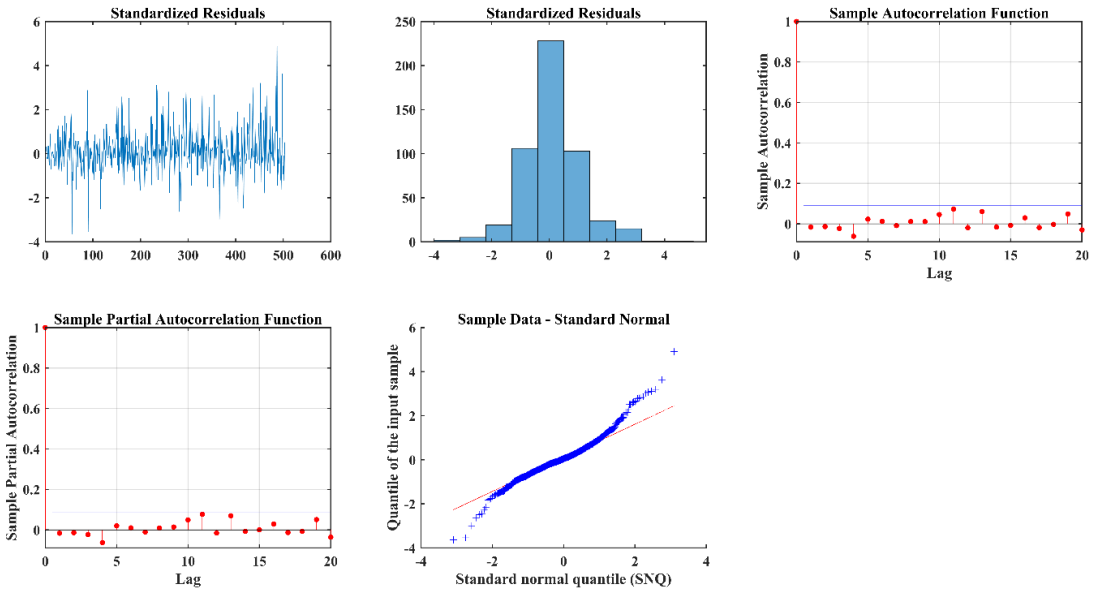

Fig. S9. Diagnostic results of SARIMA sample.